Available online at www.sciencedirect.com

ScienceDirect

Procedia Engineering 213 (2018) 392–402

Procedia Engineering

www.elsevier.com/locate/procedia

7th International Conference on Fatigue Design, Fatigue Design 2017, 29-30 November 2017, Senlis, France

The Peak Stress Method to assess the fatigue strength of welded joints using linear elastic finite element analyses

Giovanni Meneghetti[a]*, Alberto Campagnolo[a]

[a] *Department of Industrial Engineering, University of Padova, Via Venezia, 1 – 35131 Padova (Italy)*

Abstract

In fatigue design of welded joints according to the notch stress intensity factor (NSIF) approach, the weld toe profile is assumed to be a sharp V-notch having tip radius equal to zero, while the root side is assumed to be a pre-crack in the structure. The Peak Stress Method (PSM) is an engineering, FE-oriented method to estimate the NSIFs starting from the singular linear elastic peak stresses calculated at the V-notch or crack tips by using a coarse FE mesh. The element type is kept constant and the average element size can be chosen arbitrarily within a given range. The method is used in conjunction with Ansys software. The FE meshes are claimed to be coarse in comparison to those necessary to evaluate the NSIFs from the local stress distributions. Two-dimensional as well as three dimensional FE analyses can be adopted to apply the method. By using the averaged Strain Energy Density (SED, which can be expressed as a function of the relevant NSIFs) as a fatigue strength criterion, a so-called equivalent peak stress is defined to assess either weld toe or weld root fatigue failures in conjunction with a properly calibrated design curve. After presenting the theoretical background of the method, the paper presents a review of applications of the PSM relevant to steel welded joints under uniaxial as well as multiaxial fatigue loadings. Because of the relatively coarse FE analyses required and simplicity of post-processing the calculated peak stresses, the PSM might be useful in the everyday design practice.

Peer-review under responsibility of the scientific committee of the 7th International Conference on Fatigue Design.

Keywords: Fatigue; Steel welded joints; Peak stress method (PSM); Strain energy density (SED), Coarse mesh

* Corresponding author. Tel.: 0039 049 8276751; fax: 0039 049 8276785.
E-mail address: giovanni.meneghetti@unipd.it

1877-7058
Peer-review under responsibility of the scientific committee of the 7th International Conference on Fatigue Design.
10.1016/j.proeng.2018.02.039

1. Introduction: NSIF-based local approaches

The Standards and Recommendations relevant to the fatigue design of steel welded joints [1,2] suggest structural engineers to perform the fatigue strength assessment following different procedures: those based on S-N curves by adopting the nominal, the structural hot-spot or the notch stresses, or that based on the Linear Elastic Fracture Mechanics (LEFM). These approaches have the advantage to be quite easy and rapid to apply, however, concerning the assessment capability, it is well known in the literature that local approaches, such as those based on Notch Stress Intensity Factors (NSIFs), provide the best level of accuracy.

In the fatigue design of welded joints, the NSIF-based approaches assume both the weld toe and the weld root as sharp V-notches, having a notch tip radius $\rho = 0$, according to a worst case hypothesis, and notch opening angle greater than zero (typically 135°) and equal to zero, respectively, as shown in Fig. 1 [3,7]. Then singular, linear elastic stress fields in the vicinity of the notch tip can be quantitatively described by means of the relevant NSIFs,. NSIFs can be defined according to Gross and Mendelson [8] by means of Eq. (1):

$$K_i = \sqrt{2\pi} \cdot \lim_{r \to 0} \left[\left(\sigma_{jk} \right)_{\theta=0} \cdot r^{1-\lambda_i} \right] \quad \text{where} \quad i = 1,2,3 \quad \text{and} \quad \sigma_{jk} = \sigma_{\theta\theta}, \tau_{r\theta}, \tau_{\theta z} \ \text{respectively} \tag{1}$$

In previous expression, λ_i is the stress singularity exponent tied to mode I, II and III for i = 1, 2 and 3, respectively, and it depends on the notch opening angle 2α (see Tables 1,2), while the stress components $\sigma_{\theta\theta}$, $\tau_{r\theta}$ and $\tau_{\theta z}$ are calculated along the notch bisector line (θ=0).

Lazzarin et al. [9] assumed the strain energy density averaged over a structural volume surrounding the weld root or the weld toe as a fatigue strength criterion. They assumed a structural volume having circular shape with radius R_0 and provided the closed-form expression of the averaged SED parameter as a function of the relevant NSIFs. Dealing with a general multiaxial fatigue loading condition (mixed mode I+II+III loading, see Fig. 1), the SED averaged over the control volume can be expressed as follows [9]:

$$\Delta\overline{W} = c_{w1} \frac{e_1}{E} \left[\frac{\Delta K_1}{R_0^{1-\lambda_1}} \right]^2 + c_{w2} \frac{e_2}{E} \left[\frac{\Delta K_2}{R_0^{1-\lambda_2}} \right]^2 + c_{w3} \frac{e_3}{E} \left[\frac{\Delta K_3}{R_0^{1-\lambda_3}} \right]^2 \tag{2}$$

where E is the Young's modulus, e_1, e_2 and e_3 are known parameters which depend on the notch opening angle 2α and on the Poisson's ratio ν, while ΔK_1, ΔK_2 and ΔK_3 are the ranges of the NSIFs (maximum value minus minimum value) relevant to mode I, II and III, respectively. Tables 1-2 report the values of e_1, e_2 and e_3, respectively, for selected notch opening angles 2α and with reference to a Poisson's ratio $\nu = 0.3$ (structural steels) [9]. Dealing with arc-welded joints made of structural steel, the control radius R_0 was calibrated and found to be 0.28 mm [10]. Finally, the coefficients c_{wi} (i = 1, 2, 3 indicates the loading mode) depend on the nominal load ratio R according to the following expression [6]:

$$c_w(R) = \begin{cases} \dfrac{1+R^2}{(1-R)^2} & \text{if} \quad -1 \le R \le 0 \\ \dfrac{1-R^2}{(1-R)^2} & \text{if} \quad 0 \le R < 1 \end{cases} \tag{3}$$

In particular, the parameter c_w equals 0.5 for $R = -1$ and 1 for $R = 0$. It should be noted that welded joints loaded in the as-welded conditions are almost not sensitive to mean stresses, according to design standards [1], therefore Eq. (2) with $c_{wi} = 1$ should be applied.

While Lazzarin and co-workers underlined that the averaged SED can be calculated directly by FEM adopting coarse meshes within the control volume characterized by a radius R_0 [11], the Peak Stress Method (PSM) may be used to estimate the NSIFs by FEM adopting even coarser meshes [12] without modeling the control volume. Moreover, the PSM requires only the singular, linear elastic peak stresses evaluated at the V-notch tip, instead of a number of stress-distance numerical results, as required in order to calculate NSIFs on the basis of their definitions, Eq. (1).

2. The Peak Stress Method

Inspired by a numerical procedure proposed by Nisitani and Teranishi [13,14] to rapidly estimate the mode I SIF of a crack emanating from an ellipsoidal cavity, essentially, the PSM allows to rapidly estimate the NSIFs K_1, K_2 and K_3 from the singular, linear elastic, opening, sliding and anti-plane FE peak stresses $\sigma_{\theta\theta,\theta=0,peak}$, $\tau_{r\theta,\theta=0,peak}$ and $\tau_{\theta z,\theta=0,peak}$, respectively, which are referred to the V-notch bisector line (see the example in Fig. 1). The relevant expressions are as follows [12,15,16]:

$$K_{FE}^{*} = \frac{K_1}{\sigma_{\theta\theta,\theta=0,peak} \cdot d^{1-\lambda_1}} \cong 1.38 \tag{4}$$

$$K_{FE}^{**} = \frac{K_2}{\tau_{r\theta,\theta=0,peak} \cdot d^{1-\lambda_2}} \cong 3.38 \tag{5}$$

$$K_{FE}^{***} = \frac{K_3}{\tau_{\theta z,\theta=0,peak} \cdot d^{1-\lambda_3}} \cong 1.93 \tag{6}$$

In previous expressions, *d* is the so-called 'global element size' parameter to input in ANSYS® software, i.e. the mean size of the finite elements adopted by the free mesh generation algorithm available in the FE code. In the original papers, the 'exact' K_1, K_2 and K_3 NSIFs values in Eqs. (4)-(6) were derived from definitions of NSIFs, Eq. (1), applied to the stress-distance numerical results obtained from very refined FE mesh patterns (size of the smallest element close to the V-notch tip on the order of 10^{-5} mm). The average values of 1.38, 3.38 and 1.93 provided by Eqs. (4), (5) and (6), respectively, were derived under the conditions reported in Table 3 and discussed in more detail in the relevant literature [12,15,16], to which the reader is referred.

It should be noted that the mesh patterns according to the PSM, like that shown in Fig. 1, are automatically generated by the free mesh generation algorithm available in ANSYS® software, so that only the 'global element size' parameter *d* must be input by the FE analyst. There are not additional parameters or special settings to input in order to generate the mesh.

Table 1: Values of constants and of parameter f_{w1} and f_{w3} according to Eq. (9) with $\nu = 0.3$.

2α (deg)	λ_1 [(a)]	e_1 [(b)]	$R_0 = 0.28$ mm		λ_3 [(a)]	e_3 [(c)]	$R_0 = 0.28$ mm	
			$f_{w1,d=0.5mm}$ [(b)]	$f_{w1,d=1mm}$ [(b)]			$f_{w3,d=0.5mm}$ [(c)]	$f_{w3,d=1mm}$ [(c)]
0	0.500	0.133	0.997	1.410	0.500	0.414	2.459	3.478
90	0.544	0.145	1.015	1.392	0.666	0.310	1.933	2.436
120	0.616	0.129	0.918	1.198	0.750	0.276	1.737	2.065
135	0.674	0.118	0.849	1.064	0.800	0.259	1.634	1.877

[(a)]: values from [9]; [(b)]: values calculated with K_{FE}^{*} =1.38; [(c)]: values calculated with K_{FE}^{***} = 1.93

Table 2: Values of constants and of parameter f_{w2} according to Eq. (9) with $\nu = 0.3$.

2α (deg)	λ_2 [(a)]	e_2 [(b)]	$R_0 = 0.28$ mm	
			$f_{w2,d=0.5mm}$ [(b)]	$f_{w2,d=1mm}$ [(b)]
0	0.500	0.340	3.904	5.522

[(a)]: value from [9]; [(b)]: values calculated with K_{FE}^{**} = 3.38

Equations (4)-(6) are useful for a design engineer, since they allow to rapidly estimate the NSIFs K_1, K_2 and K_3 by taking advantage of the FE peak stresses $\sigma_{\theta\theta,\theta=0,peak}$, $\tau_{r\theta,\theta=0,peak}$ and $\tau_{\theta z,\theta=0,peak}$, respectively. Obviously, Eqs. (4)-(6) should be recalibrated if FE meshes with higher-order finite elements or significantly different mesh patterns as compared to the reference one (reported in Fig. 1) were adopted.

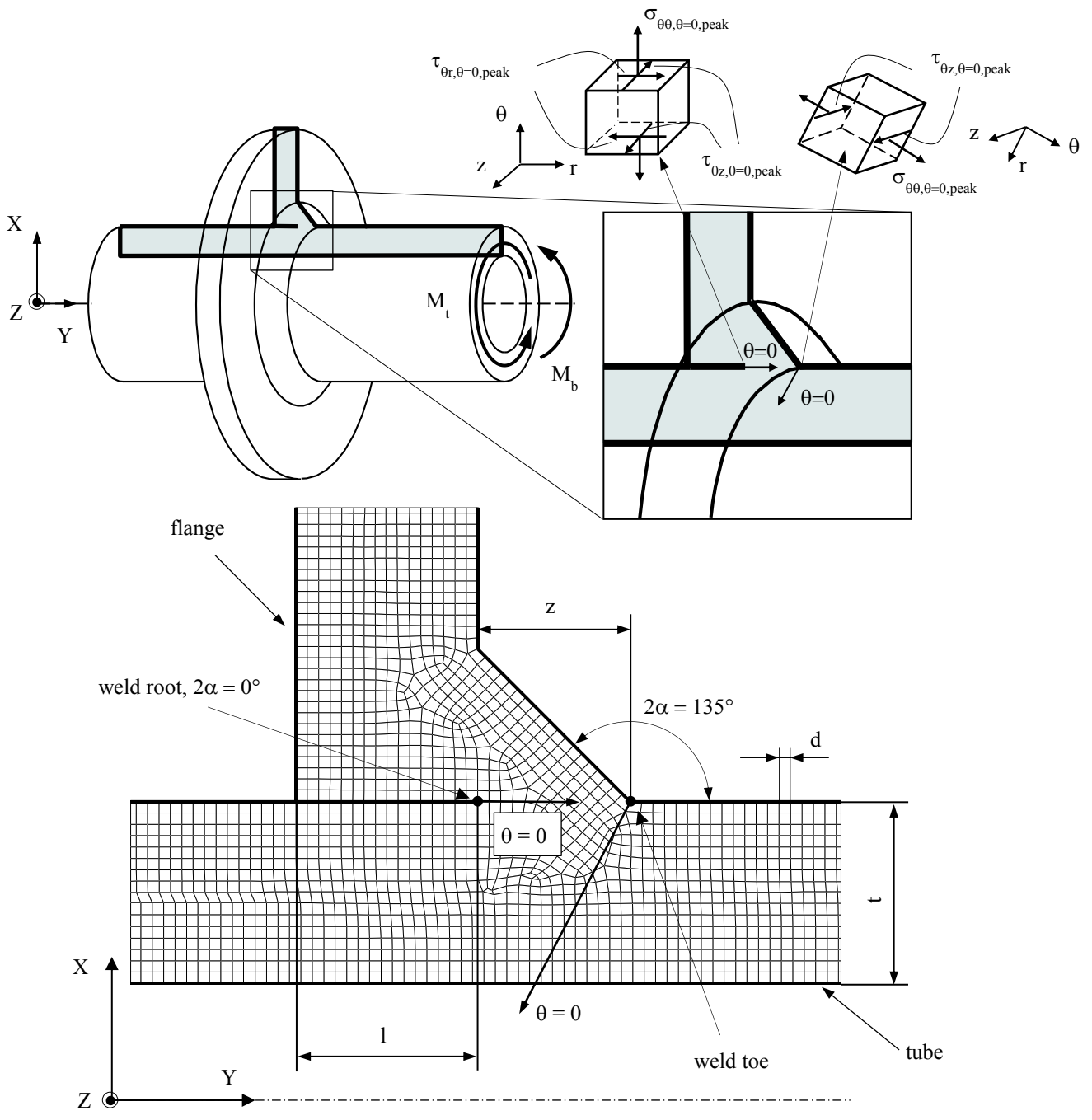

Figure 1: Typical 2D FE mesh to apply the PSM according to Eqs. (4), (5) and (6); the example reported in the figure shows a tube-to-flange fillet welded joint under multiaxial bending-torsion (M_b - M_t) loading, which has been reanalysed according to PSM in [17]. The four-node, quadrilateral, harmonic PLANE 25 elements available in Ansys® Element Library were adopted to generate the free mesh shown in the figure. The Y-axis coincides with the axis of the tube.

Table 3. Conditions for applicability of Eqs. (4)-(6) by using ANSYS® FE code [12,15,16].

	Loading mode		
	Mode I	Mode II	Mode III
Eq.	(4)	(5)	(6)
K_{FE}	1.38 ± 3%	3.38± 3%	1.93± 3%
2D FE^	PLANE 42 or PLANE 182 (K-option 1 set to 3)		PLANE 25
3D FE^	SOLID 45 or SOLID 185 (K-option 2 set to 3)		
Mesh pattern	4 elements share the node at the notch tip if $2\alpha \le 90°$ (typically at the weld root) 2 elements share the node at the notch tip if $2\alpha > 90°$ (typically at the toe side)		
2α	$0° \le 2\alpha \le 135°$	$2\alpha = 0°$	$0° \le 2\alpha \le 135°$
Minimum a/d	3	14	3 (toe, $2\alpha \cong 135°$) 12 (root, $2\alpha = 0°$)
a – root side°	$a = \min\{l, z\}$	$a = \min\{l, z\}$	$a = \min\{l, z, t\}$
a – toe side°	$a = t$	-	$a = t$

^ finite elements of Ansys® Element Library
° l, z, t are defined in Fig. 1

3. Defining a SED-based design stress using the PSM

By using the PSM-based relationships (Eqs. (4)-(6)), the closed-form expression of the averaged SED, Eq. (2), can be rewritten as a function of the singular, linear elastic FE peak stresses $\sigma_{\theta\theta,\theta=0,peak}$, $\tau_{r\theta,\theta=0,peak}$ and $\tau_{\theta z,\theta=0,peak}$. Then, by considering the strain energy equality $W = \left(1-\nu^2\right)\cdot \sigma_{eq,peak}^2 / 2E$ valid under plane strain conditions, the following equivalent peak stress, $\sigma_{eq,peak}$, can be derived:

$$\Delta\overline{W} = c_{w1}\frac{e_1}{E}\left[K_{FE}^{*}\cdot\Delta\sigma_{\theta\theta,\theta=0,peak}\cdot\left(\frac{d}{R_0}\right)^{1-\lambda_1}\right]^2 + c_{w2}\frac{e_2}{E}\left[K_{FE}^{**}\cdot\Delta\tau_{r\theta,\theta=0,peak}\cdot\left(\frac{d}{R_0}\right)^{1-\lambda_2}\right]^2 + c_{w3}\frac{e_3}{E}\left[K_{FE}^{***}\cdot\Delta\tau_{\theta z,\theta=0,peak}\cdot\left(\frac{d}{R_0}\right)^{1-\lambda_3}\right]^2 \rightarrow = \frac{1-\nu^2}{2E}\Delta\sigma_{eq,peak}^2 \quad (7)$$

Afterward, the following expression is obtained for a general multiaxial loading condition [17,18]:

$$\Delta\sigma_{eq,peak} = \sqrt{c_{w1}\cdot f_{w1}^2\cdot\Delta\sigma_{\theta\theta,\theta=0,peak}^2 + c_{w2}\cdot f_{w2}^2\cdot\Delta\tau_{r\theta,\theta=0,peak}^2 + c_{w3}\cdot f_{w3}^2\cdot\Delta\tau_{\theta z,\theta=0,peak}^2} \quad (8)$$

The correction parameters f_{w1}, f_{w2} and f_{w3} weight the peak stresses both around the notch tip and along the radial direction, i.e. θ and r coordinates, respectively, in Fig. 1. The coefficients f_{w1}, f_{w2} and f_{w3} are defined as following:

$$f_{wi} = K_{FE}\cdot\sqrt{\frac{2e_i}{1-\nu^2}}\cdot\left(\frac{d}{R_0}\right)^{1-\lambda_i} \qquad \text{where} \quad i = 1,2,3 \quad (9)$$

Tables 1 and 2 report the values of f_{w1}, f_{w2} and f_{w3}, respectively, according to Eq. (9) taking into account two values of the mean FE size, d = 0.50 mm and 1 mm, different notch opening angles 2α and a control radius for SED evaluation R_0 = 0.28 mm, valid for joints made of structural steels [10]. It should be noted that while both the parameters f_{w1}, f_{w2} and f_{w3} and the peak stresses of Eq. (8) depend on the adopted FE size d, the equivalent peak stress does not.

4. Structural steels joints: geometries and FE stress analyses according to the Peak Stress Method

A large bulk of experimental fatigue data, approximately 1300, concerning welded joints subjected to pure axial, pure bending, pure torsion and multiaxial fatigue loadings have been reanalysed by using the PSM. All joints were made of structural steels by arc-welding. Table 4 reports the geometries of considered joints subjected to pure mode

I or mode I+II loading conditions: plane geometries have been reanalysed by means of 2D FE analyses in [12,15,19–21], while 3D models have been adopted in [22,23] for more complex geometries, which could not be analysed with 2D models. Then, Table 5 reports the considered joint geometries subjected to pure mode III or multiaxial I+II+III loading conditions: the test data obtained under pure torsion have been reanalysed in [16,24], while those obtained under multiaxial in-phase as well as out-of-phase fatigue loadings have been reanalysed in [17,18]. For details about materials, welding processes and testing conditions, the reader is referred to the relevant literature [12,15–24].

For the sake of brevity, only few details about the analysis procedure according to PSM are reported here. When dealing with 2D joint geometries under axial or bending loadings, a free mesh pattern of 2D quadrilateral four-node solid elements (PLANE 42 or PLANE 182 of the ANSYS® element library), was used to evaluate the peak stresses either at the weld root or at the weld toe sides. When axis-symmetric joints under bending or torsion loadings were under consideration, a free mesh pattern of 2D quadrilateral four-node harmonic elements (PLANE 25 of the ANSYS® element library) was adopted, as shown in the example of Fig. 1. Concerning more complex joint geometries which cannot be analysed with 2D models, 3D FE analyses have been performed to calculate peak stresses according to the three-dimensional PSM as described in more detail in [22]. More precisely, first a FE analysis of the whole joint geometry was carried out by means of a main model; subsequently, a submodel of the critical area of the joint (the weld toe or weld root) was analysed by adopting the submodelling technique available in Ansys® software. The main model was meshed by employing a free mesh of second-order, ten-node tetra elements (SOLID 95 or equivalently SOLID 187 of the Ansys® element library). Then, the submodel was defined by cutting the main model at a distance from the weld toe (or the weld root) equal to one main plate or tube thickness. To obtain the 3D mesh of the submodel, a 2D free mesh pattern of quadrilateral four-node PLANE 182 elements having average size d was generated in order to obtain the standard 2D mesh pattern required by the PSM (according to Fig. 1); subsequently, the 2D FE mesh was extruded by setting an extrusion step size equal to the average element size d and by using 3D eight-node brick elements (SOLID45 of the Ansys® element library or equivalently SOLID185 with K-option 2 set to 3).

5. Assessment of weld toe and weld root fatigue failures

The fatigue experimental results relevant to joint geometries reported in Tables 4 and 5 have been reconverted in [12,15–24] in terms of equivalent peak stress, Eq. (8), evaluated at the point of crack initiation (either the toe or the root) as observed experimentally.

The experimental results obtained from steel welded joints subjected to pure mode I or mode I+II loading conditions have been compared in Fig. 2a with the fatigue design scatter band previously calibrated in [19] on test data generated by weld toe failures in T or cruciform steel welded joints subjected to axial or bending loadings in the as-welded conditions and with a nominal load ratio R close to zero. It can be observed from Fig. 2a that the agreement between the design scatter band and about 980 experimental results generated from both weld toe and weld root failures in joints tested in the as-welded as well as stress relieved conditions, is satisfactory.

Figure 2b shows the comparison between the experimental results obtained from steel welded joints subjected to pure mode III loading conditions and the fatigue design scatter band, which has been previously calibrated in [16] on experimental results relevant only to weld toe failures in full penetration tube-to-flange steel joints tested under pure torsion loading in the stress-relieved condition and with a nominal load ratio R equal to -1. A fairly good agreement can be observed in Fig. 2b between the fatigue design scatter band and about 150 experimental results generated from both weld toe and weld root failures in steel joints tested in the as-welded as well as stress relieved conditions.

Finally, the experimental data obtained from structural steel joints subjected to mode I+III or the most general mode I+II+III loading conditions have been compared in Fig. 2c with the scatter band suggested in [17] to design steel welded joints against multiaxial fatigue. Figure 2c shows that in most cases a good agreement between theoretical estimations based on PSM and about 150 experimental fatigue results has been obtained for joints tested under multiaxial in-phase as well as out-of-phase fatigue loadings.

Table 4: Joint geometries subjected to pure mode I or mode I+II loading conditions reanalysed according to PSM, Eq. (8), by means of 2D [12,15,19–21] or 3D [22,23] FE analyses with coarse meshes.

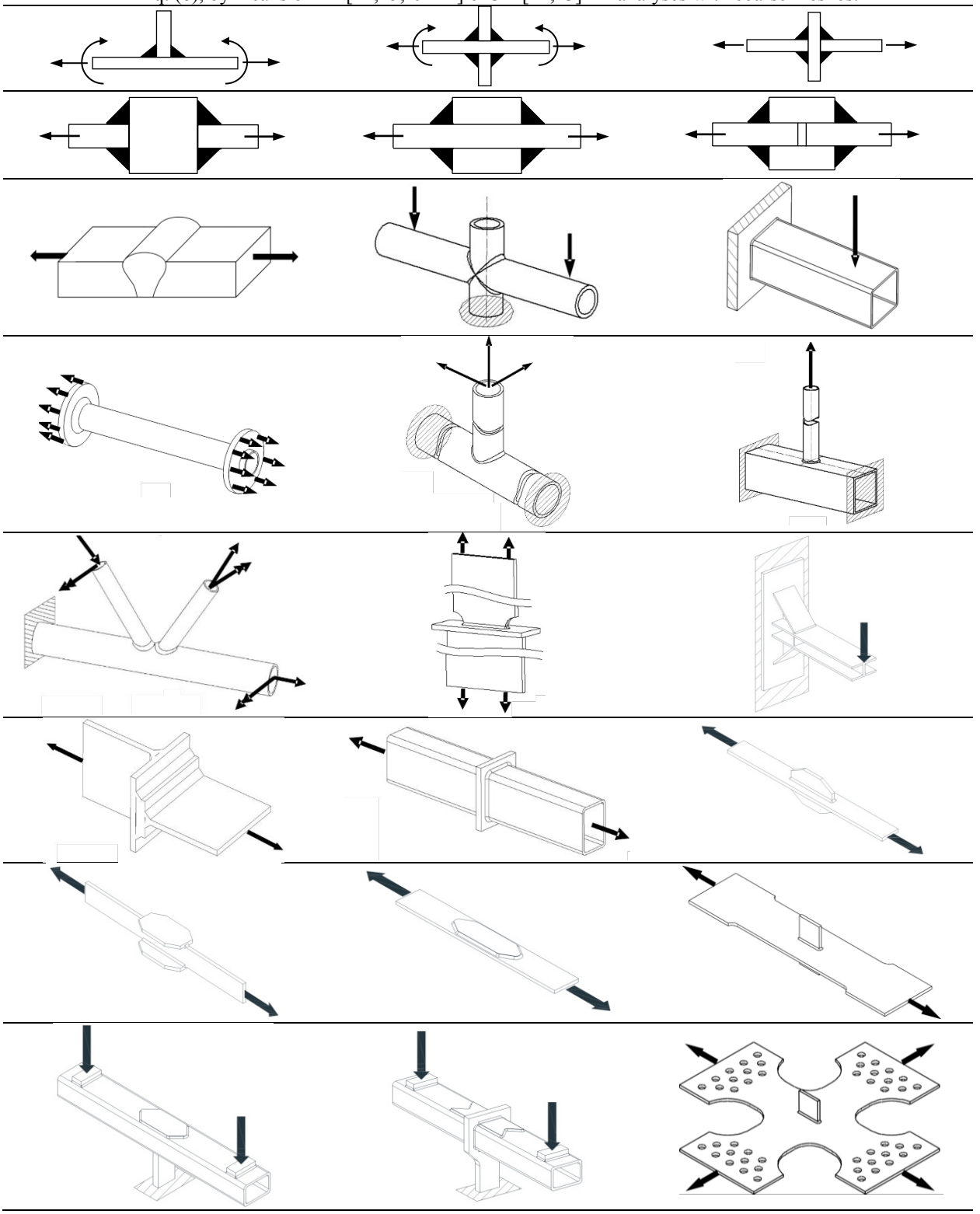

Table 5: Joint geometries subjected to pure mode III [16,24] or multiaxial mode I+III or mode I+II+III [17,18] loading conditions reanalysed according to PSM, Eq. (8), by means of 2D or 3D FE analyses with coarse meshes.

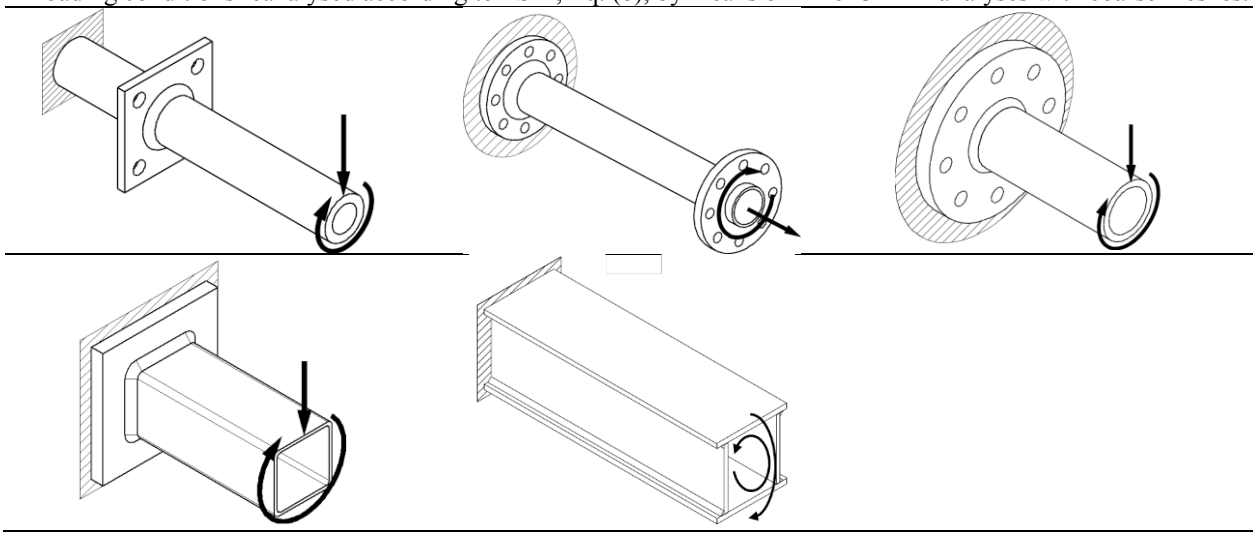

Dealing with steel joints tested under pure torsion or multiaxial fatigue loadings in the as-welded conditions, a general conservatism has been observed in Figs. 2b and 2c between theoretical estimations and experimental results. One of the reasons for this result could be due to the presence of compressive residual stresses at the weld toe and root sides, which have been measured for example by Yung and Lawrence [25] in tube-to-flange welded joints. In particular, they noted that fatigue strength was decreased after performing the post-welding heat treatment to relieve residual stresses. The reader is referred to the relevant literature [16,17,24] for more detailed discussions about these phenomena.

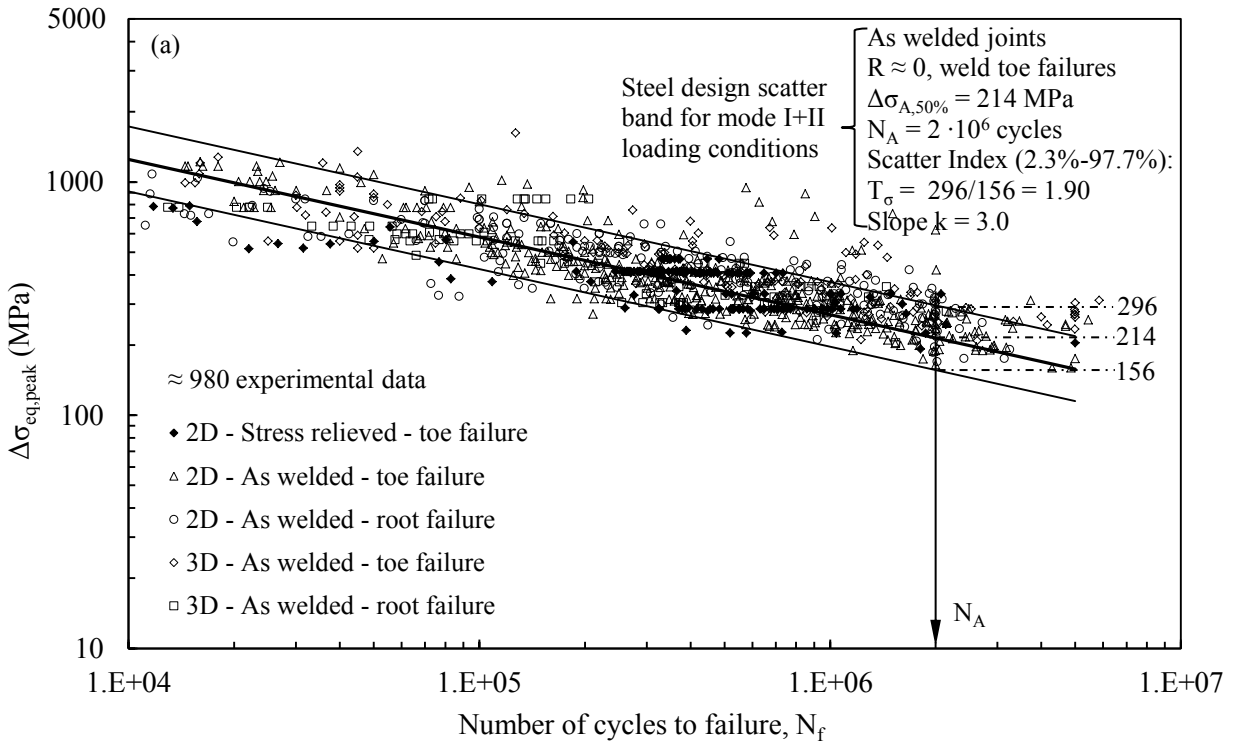

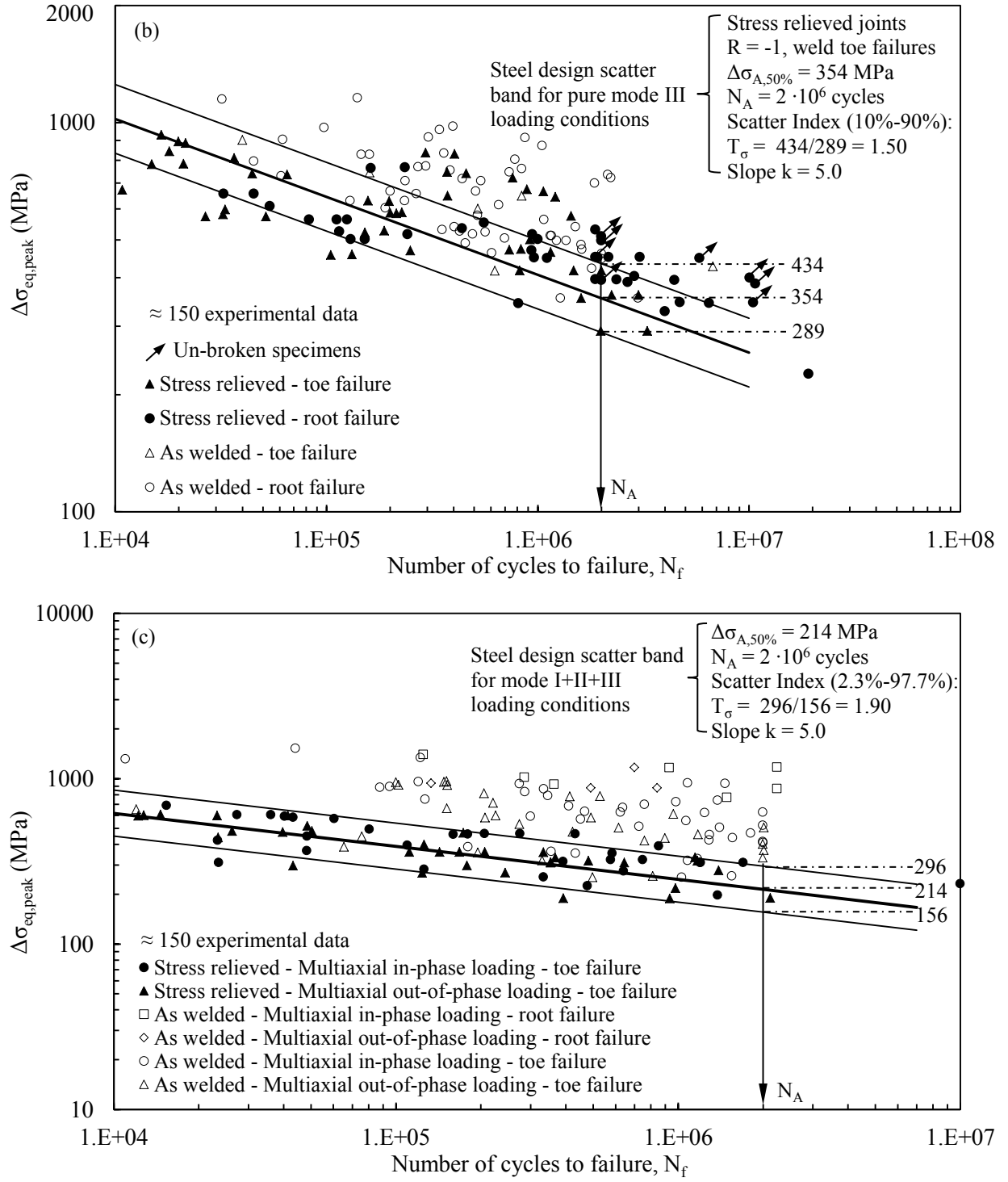

Figure 2: Fatigue assessment of structural steel welded joints (Tables 4 and 5) according to the PSM. Comparison between the fatigue design scatter band and experimental fatigue results obtained under (a) mode I+II, (b) mode III and (c) mode I+II+III loading conditions.

6. Conclusions

The peak stress method (PSM) is based on the NSIF approach and employs the singular, linear elastic peak stresses evaluated at the toe and root sides by means of FE analyses with coarse meshes. A properly defined design stress, the so-called equivalent peak stress, has been adopted to assess weld toe as well as weld root fatigue failures in several 2D and 3D joint geometries tested under axial, bending, torsion as well as multiaxial fatigue loadings, both in-phase and out-of-phase. All in all, approximately 1300 experimental data have been considered. Comparison between experimental fatigue results and the relevant design scatter bands was satisfactory. Because of the simplicity of a point-like method combined with the robustness of the NSIF approach, the PSM might be useful to design engineers engaged in fatigue assessments of welded joints.

References

[1] Eurocode 3: Design of steel structures – part 1–9: Fatigue, CEN, 2005.

[2] A.F. Hobbacher, Recommendations for Fatigue Design of Welded Joints and Components, IIW Collection. Springer International Publishing, 2016.

[3] P. Lazzarin, R. Tovo, A notch intensity factor approach to the stress analysis of welds, Fat. Fract. Eng. Mater. Struct. 21 (1998) 1089–1103.

[4] P. Lazzarin, P. Livieri, Notch stress intensity factors and fatigue strength of aluminium and steel welded joints, Int. J. Fatigue. 23 (2001) 225–232.

[5] P. Lazzarin, T. Lassen, P. Livieri, A notch stress intensity approach applied to fatigue life predictions of welded joints with different local toe geometry, Fatigue Fract. Eng. Mater. Struct. 26 (2003) 49–58.

[6] P. Lazzarin, C.M. Sonsino, R. Zambardi, A notch stress intensity approach to assess the multiaxial fatigue strength of welded tube-to-flange joints subjected to combined loadings, Fatigue Fract. Eng. Mater. Struct. 27 (2004) 127–140.

[7] D. Radaj, C.M. Sonsino, W. Fricke, Fatigue Assessment of Welded Joints by Local Approaches, Woodhead Publishing, Cambridge, 2006.

[8] B. Gross, A. Mendelson, Plane elastostatic analysis of V-notched plates, Int. J. Fract. Mech. 8 (1972) 267–276.

[9] P. Lazzarin, P. Livieri, F. Berto, M. Zappalorto, Local strain energy density and fatigue strength of welded joints under uniaxial and multiaxial loading, Eng. Fract. Mech. 75 (2008) 1875–1889.

[10] P. Livieri, P. Lazzarin, Fatigue strength of steel and aluminium welded joints based on generalised stress intensity factors and local strain energy values, Int. J. Fract. 133 (2005) 247–276.

[11] P. Lazzarin, F. Berto, M. Zappalorto, Rapid calculations of notch stress intensity factors based on averaged strain energy density from coarse meshes: Theoretical bases and applications, Int. J. Fatigue. 32 (2010) 1559–1567.

[12] G. Meneghetti, P. Lazzarin, Significance of the elastic peak stress evaluated by FE analyses at the point of singularity of sharp V-notched components, Fatigue Fract. Eng. Mater. Struct. 30 (2007) 95–106.

[13] H. Nisitani, T. Teranishi, KI value of a circumferential crack emanating from an ellipsoidal cavity obtained by the crack tip stress method in FEM, in: M. Guagliano, M.H. Aliabadi (Eds.), Proc. 2nd Int. Conf. Fract. Damage Mech., 2001: pp. 141–146.

[14] H. Nisitani, T. Teranishi, KI of a circumferential crack emanating from an ellipsoidal cavity obtained by the crack tip stress method in FEM, Eng. Fract. Mech. 71 (2004) 579–585.

[15] G. Meneghetti, The use of peak stresses for fatigue strength assessments of welded lap joints and cover plates with toe and root failures, Eng. Fract. Mech. 89 (2012) 40–51.

[16] G. Meneghetti, The peak stress method for fatigue strength assessment of tube-to-flange welded joints under torsion loading, Weld. World. 57 (2013) 265–275.

[17] G. Meneghetti, A. Campagnolo, D. Rigon, Multiaxial fatigue strength assessment of welded joints using the Peak Stress Method – Part II: Application to structural steel joints, Int. J. Fatigue. 101 (2017) 343–362.

[18] G. Meneghetti, A. Campagnolo, D. Rigon, Multiaxial fatigue strength assessment of welded joints using the Peak Stress Method – Part I: Approach and application to aluminium joints, Int. J. Fatigue. 101 (2017) 328–342.

[19] G. Meneghetti, P. Lazzarin, The Peak Stress Method for Fatigue Strength Assessment of welded joints with weld toe or weld root failures, Weld. World. 55 (2011) 22–29..

[20] G. Meneghetti, The Peak Stress Method Applied to Fatigue Strength Assessments of Load Carrying Transverse Fillet Welds with Toe or Root Failures, Struct. Durab. Heal. Monit. 8 (2012) 111–130.

[21] G. Meneghetti, A. Campagnolo, F. Berto, Fatigue strength assessment of partial and full-penetration steel and aluminium butt-welded joints according to the peak stress method, Fatigue Fract. Eng. Mater. Struct. 38 (2015) 1419–1431.

[22] G. Meneghetti, C. Guzzella, B. Atzori, The peak stress method combined with 3D finite element models for fatigue assessment of toe and

root cracking in steel welded joints subjected to axial or bending loading, Fatigue Fract. Eng. Mater. Struct. 37 (2014) 722–739.

[23] G. Meneghetti, D. Marini, V. Babini, Fatigue assessment of weld toe and weld root failures in steel welded joints according to the peak stress method, Weld. World. 60 (2016) 559–572.

[24] G. Meneghetti, A. De Marchi, A. Campagnolo, Assessment of root failures in tube-to-flange steel welded joints under torsional loading according to the Peak Stress Method, Theor. Appl. Fract. Mech. 83 (2016) 19–30.

[25] J.Y. Yung, F. V Lawrence, Predicting the fatigue life of welds under combined bending and torsion, in: M. Brown, K. Miller (Eds.), Biaxial Multiaxial Fatigue EGF 3., Mechanical Engineering Publications, London, 1989: pp. 53–69.